On the resistive switching mechanism of parylene-based memristive devices

Anton A. Minnekhanov[a,**], Boris S. Shvetsov[a,b], Mikhail M. Martyshov[b], Kristina E. Nikiruy[a,c], Elena V. Kukueva[a], Mikhail Yu Presnyakov[a], Pavel A. Forsh[a,b], Vladimir V. Rylkov[a,d], Victor V. Erokhin[a,e], Vyacheslav A. Demin[a], Andrey V. Emelyanov[a,c,*]

Abstract

Parylene is a widely used polymer possessing such advantages as low cost and safety for the human body. Recently, several studies have been conducted showing that parylene can be used as a dielectric layer of memristors — new circuit design elements that are promising for the implementation of hardware neural net- works. However, the mechanism of resistive switching of parylene-based memristors remains unclear. In this paper, we report the result of a comprehensive study of this mechanism for Metal/Parylene/ITO sandwich memristive devices. The obtained results clearly show that the origin of resistive switching in the devices is the formation of conductive metal bridges (filaments) from the top electrode (Cu, Ag or Al) to the bottom one (ITO). And furthermore, conductance quantization effect with both integer and half-integer multiples of the quantum of conductance $G_0 = 2e^2/h$ has been observed in the samples, which also confirms the chosen switching model, and can be useful in the development of multilevel data memory cells.

1. Introduction

Memristive devices have attracted significant attention as potential candidates for next generation nonvolatile memories that are applicable both in neuromorphic systems [1–6] and in reconfigurable and “wearable” electronics [2–4,7–9]. This interest is due to a number of their advantages, such as simple two terminal structure and scalability (down to 2 nm [10]), as well as low energy consumption and voltage operation, high write/read rate and multilevel resistive switching (RS) [2,3]. The multilevel character of RS, or the possibility of resistance variation in a window between low- and high-resistance states (R_{on}, R_{off}), is a key property of memristors for emulating synapses in the development of neuromorphic computing systems [2,3]. RS is observed in a variety of materials such as inorganic oxides (TiO_x, HfO_x, SiO_x, TaO_x, etc.) [11–17] and nitrides (Si_3N_4) [18], organic (polyaniline, parylene) [19–22] and nanocomposite [23] structures. Most memristive devices operate through the electromigration of oxygen vacancies in oxides with the subsequent formation (rupture) of conductive filaments (valence change mechanism, or VCM) or through the metal bridge growth (destruction) by means of cation motion in a dielectric matrix (electrochemical metallization, or ECM) [1]. In the last case one could achieve a wide window of RS ($R_{off}/R_{on} > 10^4$) which is preferable for neuromorphic applications [10]. In such devices an electrochemically active metal (e.g. Ag or Cu) is used as one of the electrodes of the memristive structure of metal-insulator-metal (MIM) type. Under ap- plied positive voltage cations can migrate to the cathode, where they are reduced and form metal bridges [1,7,24–31]. Observation of the formation of metal bridges is possible either directly, for example, by optical microscopy using an optically transparent organic material as a template [29], or indirectly by a variety of experimental techniques such as ion mass [27,32], X-ray photoelectron [27,33], impedance [34,35] spectroscopy methods. It is noteworthy, since such conductive filaments are quasi-one-dimensional metallic conductors, that their conductance can be quantized in integer or half-integer multiples of the quantum of conductance $G_0 = 2e^2/h$, where e is the electron charge, and h is Planck's constant [36–38].

One of the most promising memristive structures for “wearable” applications are MIM structures based on polymeric layers of parylene (poly-para-xylylene, or PPX) due to the simple and cheap production of this polymer, its transparency and the possibility of fabrication on flexible substrates [39,40]. Moreover, parylene is a US Food and Drug Administration approved material and could be used in biomedicine since it is completely safe for the human body, which cannot be said about most of the other organic materials [39,41,42]. Currently, par- ylene-based memristive structures show good memristive character- istics [39,43] including their capability of multilevel resistance switching. Moreover, recently we have demonstrated the associative learning ability of neuromorphic systems with such kind of devices [43]. However, a comprehensive study on the RS mechanisms in par- ylene-based structures has not been reported yet. At the same time an in-depth understanding of the physical mechanism underlying the RS effect is vital for optimization of memristive device performance in terms of endurance, retention time and plasticity, which could pave the way toward further development of the technology and commerciali- zation [44]. Therefore, the main goal of this work is to study electro- physical properties responsible for RS of parylene-based MIM memris- tive devices. Our study is performed using temperature dependent and quantized conductance measurements along with characterization by electron microscopy and impedance spectroscopy methods. (poly-para-xylylene, or PPX) due to the simple and cheap production of this polymer, its transparency and the possibility of fabrication on flexible substrates [39,40]. Moreover, parylene is a US Food and Drug Administration approved material and could be used in biomedicine since it is completely safe for the human body, which cannot be said about most of the other organic materials [39,41,42]. Currently, par- ylene-based memristive structures show good memristive character- istics [39,43] including their capability of multilevel resistance switching. Moreover, recently we have demonstrated the associative learning ability of neuromorphic systems with such kind of devices [43]. However, a comprehensive study on the RS

mechanisms in par- ylene-based structures has not been reported yet. At the same time an in-depth understanding of the physical mechanism underlying the RS effect is vital for optimization of memristive device performance in terms of endurance, retention time and plasticity, which could pave the way toward further development of the technology and commerciali- zation [44]. Therefore, the main goal of this work is to study electro- physical properties responsible for RS of parylene-based MIM memris- tive devices. Our study is performed using temperature dependent and quantized conductance measurements along with characterization by electron microscopy and impedance spectroscopy methods.

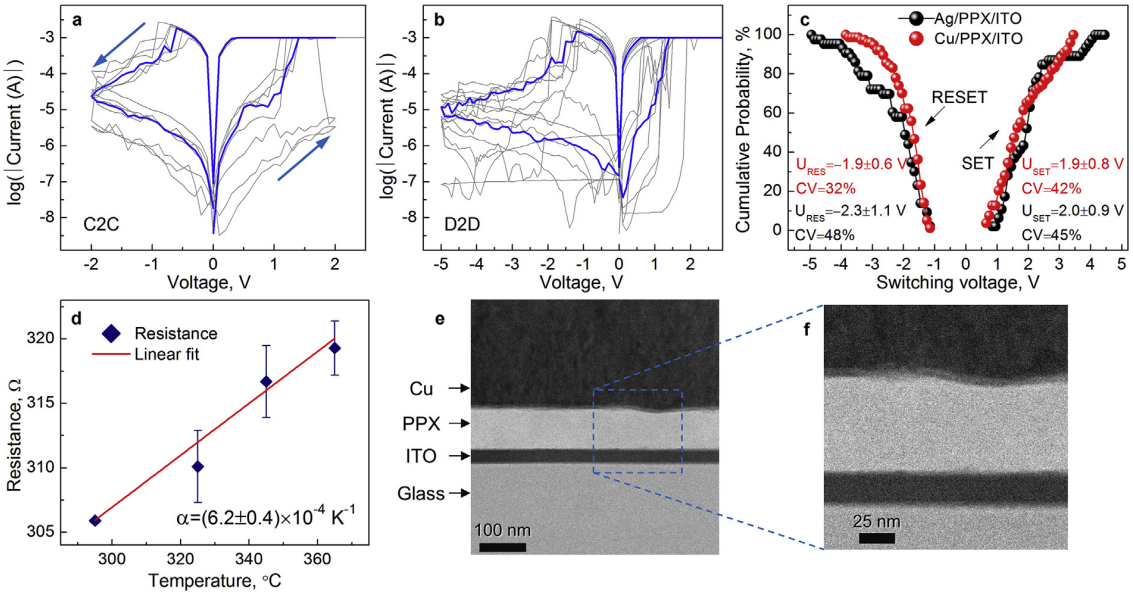

Fig. 1. Electrophysical and structural characterization of the M/PPX/ITO structures. (a) I–V sweeps showing the typical bipolar RS behavior of the Cu/PPX/ITO sample during 7 cycles (cycle-to-cycle variability); the median is highlighted in bold. (b) I–V sweeps collected in 8 different Cu/PPX/ITO devices (device-to-device variability, the 5th of 10 cycles is shown for each); the median is highlighted in bold. (c) Cumulative probabilities of U_{SET} and U_{RESET} switching voltages and their coefficients of variation (CV) for ~100 I–V sweeps measured in the samples with copper (red) and silver (black) top electrodes. (d) Temperature dependence of the LRS resistance of the Cu/PPX/ITO structure. (e) Cross-sectional TEM image of the Cu/PPX/ITO sandwich structure. (f) Enlarged image of the area highlighted by the rectangle in (e), showing roughness of the Cu/PPX interface.

2. Materials and methods

We studied memristive elements of "Metal/Parylene/Indium tin oxide" structure (further M/PPX/ITO structures). The parylene layers (~100 nm) were deposited on a commercially purchased ITO coated glass substrate (bottom electrode, or BE) by the gas phase surface polymerization method using an SCS Labcoater PDS 2010 vacuum de- position system. PDS 2010 transforms Parylene dimer (2,2-para-cyclo- phane or its derivatives) to a gaseous monomer; the material poly- merizes onto the substrate upon deposition at room temperature. At the vacuum levels employed, all sides of the substrate were uniformly im- pinged on by the gaseous monomer, resulting in a truly conformal coating. We selected ITO-coated glass as the BE because it has wide commercial availability and benefits such as high conductivity, trans- parency and resistance to moisture.

The top metal electrodes (TEs) were Ag, Al or Cu layers (~500 nm thick) obtained by thermal evaporation or ion-beam sputtering through a shadow mask. The sizes of the TEs were 0.2 × 0.5 mm^2, and about 150 single devices (per one substrate) were fabricated for each kind of electrode. The metals listed above were selected due to their wide- spread use in electronic engineering including the manufacture of memristive devices. Furthermore, we have shown recently that M/PPX/ ITO memristive structures with upper electrodes made of these metals demonstrate good performance and are applicable to the implementa- tion of neuromorphic systems [43].

The structural investigations were carried out with the transmission electron microscope (TEM) Titan 80-300 (FEI, USA) in TEM and STEM modes. An energy dispersive X-ray analyzer (EDX, USA) was used to reveal the chemical composition. The cross-sectional preparation of the memristive samples was done by the focused ion beam method on Helios 600i.

I–V curves and related electrical characteristics of the M/PPX/ITO structures were studied using a Cascade Microtech PM5 analytical probe station with a heating unit; the voltage pulses were supplied by a National Instruments PXIe-4140 source measure unit, programmed in LabView. Impedance spectroscopy studies were carried out with the HP 4192A impedance analyzer. The

measurements were performed in the frequency range from 5 Hz to 13 MHz with the amplitude of the vari- able signal of 50 mV. The capacitance of the structures was measured at the frequency of 100 kHz.

3. Experimental results

3.1. Resistive switching property

As was reported before [43], the M/PPX/ITO memristive devices have generally good performance, especially the ones with Cu TEs. Indeed, the Cu/PPX/ITO structures (which we will further denote as "Cu samples") demonstrated the R_{off}/R_{on} value of $\sim 10^3$, endurance higher than 10^3 cycles, and at least 16 stable resistive states with re- tention time>10^4 s for R_{on} = 1kΩ and R_{off} = 1MΩ. Such perfor- mance parameters made it possible to implement on the basis of the Cu sample the simplest model of the spike neuromorphic system — the electronic Pavlov's dog [43].

Fig. 1(a) depicts several consecutive I–V cycles of one Cu sample, along with their median I–V curve, which represents the so-called cycle- to-cycle (C2C) stability. (I–V curves for the Ag and Al samples can be found in SM, Fig. S1.) The measurements were carried out at room temperature under normal conditions, the external voltage was applied to the Cu TE with the ITO BE grounded. A current compliance of 1 mA was adopted to prevent a device breakdown. As one can see, the Cu/ PPX/ITO structure practically does not need a forming process and every sweep goes in a similar way. The device-to-device (D2D) curves along with their median are presented in Fig. 1(b) (the 5th of 10 cycles is shown for each sample). It is clear that the cycles for different sam- ples have a reasonable repeatability, which is also confirmed by the distribution of RS voltages U_{SET} and U_{RESET} (Fig. 1(c)). Note that this distribution is narrower (the coefficient of variation is lower) for the Cu samples compared to the Ag ones. Considering the symmetrical and repeatable behavior of the RS, it can be said that it is most likely caused by the formation of a conducting filament in the dielectric between the electrodes. In our case, it is reasonable to assume that such a conducting filament is a metal bridge consisting of atoms of the TE (formed as a result of electrochemical metallization, or ECM mechanism) [1,3]. Subsequent studies presented in this paper are intended to confirm this hypothesis.

First of all, we have studied the temperature-dependent switching characteristics of the aforementioned Cu/PPX/ITO memristive devices, which is informative for understanding the RS mechanisms. The resistance of the structure was calculated from the I–V measurements conducted in the range from 0 to 0.5 V. Fig. 1(d) shows the dependence of the LRS resistance (R_{on}) on temperature. It is clear that the resistance in LRS increases linearly with temperature, exhibiting the typical metallic conduction property. In general, the dependence of metallic resistance on temperature can be expressed as $R(T) = R\,[1 + \alpha(T - T)]$, where R_0 is the resistance at T_0 and α is the temperature coefficient of resistance (TCR). According to the experimental data (Fig. 1(d)), we have obtained the coefficient $\alpha = (0.62 \pm 0.04) \times 10^{-3}\ K^{-1}$ at 300 K. It should be noted that the TCR of Cu nanowire decreases with its diameter, probably due to surface diffuse scattering [45–47], thus we may conclude that the metallic behavior of the LRS of Cu/PPX/ITO devices originates from the small-size conducting Cu filament. We will discuss this result in more detail in the discussion section.

The TEM investigations also show the possibility of the formation of metallic bridges between the top and the bottom electrodes of the M/ PPX/ITO structures. Indeed, one can see in Fig. 1(e–f) that the copper layer is not completely smooth and the roughness of the Cu/PPX in- terface is sufficient for the metal ions to begin to migrate toward the cathode (ITO). It should be noted that we were not able to find the filament itself in the studied samples as the area of the TEs was too large for such a task. Nevertheless, given the incomplete electron microscopy results, we conducted several additional studies of the RS process in the samples, which led to interesting and somewhat unexpected results. Let us consider them.

3.2. Capacitance measurements

To further study the RS mechanism, we carried out impedance spectroscopy measurements. Fig. 2(a) depicts typical impedance ho- dographs obtained for the Al samples for their two different HRSs (so the direct current resistance R_{dc} equals 5 and 27 kΩ). The inset shows an impedance hodograph for the LRS (R_{dc} = 200 Ω). Similar de- pendences were also obtained for other stable states and for the Cu samples.

It is clear from the figure that the hodographs for the HRSs have the appearance of semicircles. On the other hand, the hodograph for the LRS is almost a vertical line, which indicates that the structure is a conductor in this state. Thus, increasing the resistance of the structure we observe its evolution from a conductor to a capacitor. This can be described by the equivalent electrical scheme, shown in the inset in Fig. 2(b). In this scheme C_d represents the capacitance of the dielectric parylene layer, the resistance R_c represents resistance of lead wires and contacts; in parallel with C_d there are the resistance R_f connected in series with the R_gC_g element, contributed to the conductive filaments and gaps in them, respectively. Such an equivalent circuit describes well the HRS of M/PPX/ITO structures — R_g is very large in this case. Further, we assume that a conductive filament (metal bridge) is formed in the dielectric layer as a result of switching to the LRS, and R_g falls down, so the current flows through it. In LRS R_g is almost zero, because the gap is absent. It should be noted that the resistance R_g can change during the evolution of the filament, which can result in the change of the whole structure's resistance. For instance, R_g should increase dra- matically along with the capacitance C_g after switching the structure back to the HRS due to the gap forming. So the total capacitance of the structure should increase. But as can be seen from Fig. 2(b), when the M/PPX/ITO structure resistance changes by several orders of magni- tude from the LRS to the HRS, its capacitance does not change within the limits of error. (Details of the capacitance measurement process are provided in SM Note 1.) A small difference in the capacitance between the samples with Cu and Al TEs can be associated with the difference in the thickness of the parylene films, which can vary in the range of 5–10%. So we can conclude that the capacitance of the gaps C_g does not impact the total capacitance C, which depends mostly on C_d in the studied frequency region. This may occur only if the total area

of all the gaps is negligible compared to the area of the TE, which indicates a small amount of conductive filaments in the sample switched to the LRS.

Thus, the obtained results confirm that the origin of RS in the M/ PPX/ITO structures is the formation of the conductive metal bridges (filaments) with a small cross-sectional area (so the capacitance C does not change). This is consistent with the results of temperature mea- surements, as well as with the data on the conductance quantization, which we will discuss in the next section. Note, if the transition from the HRS to the LRS passes through the formation of multi-filaments or metal tissue, then the change in the effective dielectric constant of the structure would be significant, which would lead, in turn, to a sig- nificant change in the sample capacitance [34,35]. Hence, RS in the samples is driven definitely by the ECM mechanism leading to the formation of a single conductive metal bridge (or a small number thereof).

3.3. Conductance quantization

As is shown in the previous sections, the bipolar RS behavior of the investigated samples most likely originates from the formation/de- struction of metal bridges in the dielectric layer due to the electro- chemical metallization process. Namely, the formation of these bridges occurs due to the migration of metal cations (Ag^{+}, Cu^{+}/Cu^{+2} or Al^{+3}) from the TE toward the BE during the SET process under strong electric field. Conversely, the conductive bridges break during the RESET switching due to the movement of metal cations in the opposite di- rection. Under these conditions nanometer-scale metallic constrictions can be formed causing quantization of the conductance [36–38].

Let us consider the M/PPX/ITO structure with a metal bridge formed as a result of a RS to the LRS. On applying a negative voltage to the TE of the structure the bridge starts to break down. It should be expected that just before the moment of the complete rupture of the metal bridge the constriction with a very small diameter will appear (an order of the Fermi wavelength of the electron in the bridge, typically nanometers). As a rule, the mean free path of the electron is greater than the length of the constriction and electrons move ballistically through it (without scattering). In this scenario, the electron transport is quantized in multiples of the fundamental conductance quantum $G_0 = 2e^2/h = 7.75 \times 10^{-5}$ S and total conductance of the structure G can be expressed as $G = nG_0$ (n = 1, 2, 3 ...) [36–38]. We clearly ob- served this process using slow-sweep (0.1 V/s, with the increment of 0.005 V) I–V measurements.

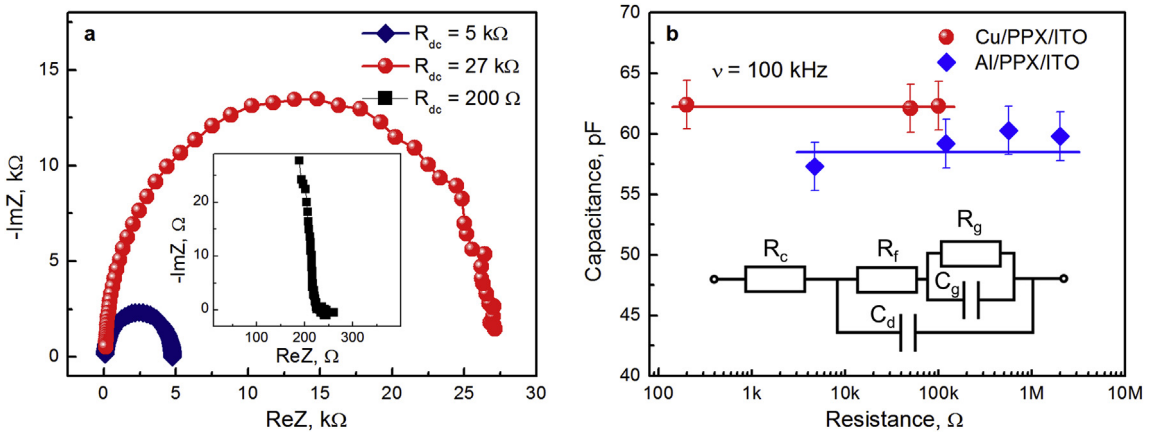

Fig. 2. Impedance spectroscopy measurements of the M/PPX/ITO structures. (a) Typical impedance hodographs for the Al/PPX/ITO samples for different resistive states R_{dc}. Inset shows an almost vertical hodograph for the LRS of the structure. (b) Capacitance vs. direct current resistance R_{dc} dependences for the Al/PPX/ITO and Cu/PPX/ITO samples. Inset shows the equivalent electrical scheme: C_d is the capacitance of the dielectric parylene layer, R_c is the resistance of lead wires and contacts, R_f is the resistance of the conductive filament, R_g and C_g are the resistance and the capacitance of the gap in the conductive filament.

As one can see from Fig. 3(a), the Cu samples show a multistep reset process. This part of I–V curve (designated with the dashed blue rec- tangle) is shown enlarged in the inset of Fig. 3(b), with the current values converted to conductance measured in units of G_0. We should note that every point of this curve takes integer multiples or, rather unexpectedly, half-integer multiples of G_0: it depicts stepwise decrease of conductance from 5 G_0 at −3.5 V to 0.5 G_0 at −4.15 V and then to ~0. At least 4 plateau conductance levels can be identified during this process: 2.5 G_0, 2 G_0, 1.5 G_0 and 0.5 G_0 at −3.8V, −3.9V, −4V and −4.15 V, respectively. In addition, to make a statistical analysis of the conductance quantization phenomenon, more than 1600 conductance values were extracted from about 10 reset processes. The corresponding histogram is shown in Fig. 3(b) along with the Gaussian fitting of the resulting peaks (the blue curve). One can see that the conductance peaks are located at both integer and half-integer multiples of G_0, with a relatively wide distribution around each peak. That agrees with physical phenomenon of conductance quantization and indicates that parylene-based memristive devices under proper conditions can be used in the relevant applications.

In general, the observed quantum effects can be expected, because, as mentioned above, the nanometer-scale constriction forms just before the rupture of the conducting bridge. It is noteworthy that similar processes were also observed in Ag and Al samples (see SM Fig. S2) in multiple devices. So there is no doubt that the conductance quantiza- tion with integer values of G_0 originates from the quantum-size con- striction in metal bridges. At the same time, the half-integer quantum conductance values are much more difficult to explain. Indeed, many studies have shown that this type of conductance quantization is a characteristic feature of a VCM mechanism rather than ECM: memris- tors with metal filaments are more likely to exhibit conductance quantization with only integer multiples of G_0 [37,38]. On the other hand, it was also shown that the dielectric medium surrounding the filament also affects its conductivity. For instance, half-integer quan- tized conductance values were observed in memristors with metal fi- laments in organic dielectric media like polyethylene oxide (PEO) [48] and P3HT:PCBM [24]. Parylene is also organic, so we have every reason to believe that our result is consistent with literature. So, we have found another strong confirmation of our hypothesis about the RS mechanism in the samples, even if it is indirect.

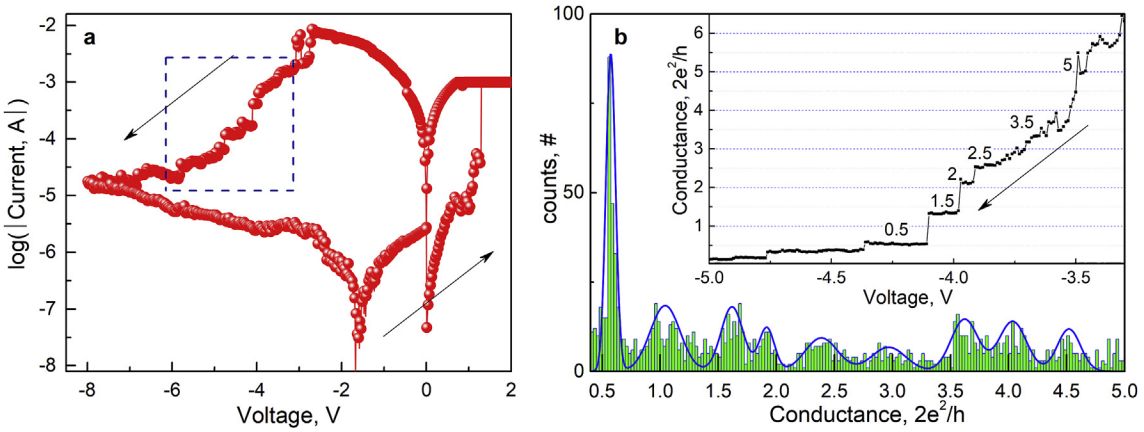

Fig. 3. (a) I–V curve for the Cu/PPX/ITO memristor. (b) Histogram of more than 1600 conductance values extracted from about 10 reset processes in the sample, measured at a sweep rate of 0.1 V/s. The Gaussian fitting curve (blue) serves as a guide to the eye. Inset shows a redrawing of the conductance quantization observed in the region indicated by blue rectangle in (a). (For interpretation of the references to colour in this figure legend, the reader is referred to the Web version of this article.)

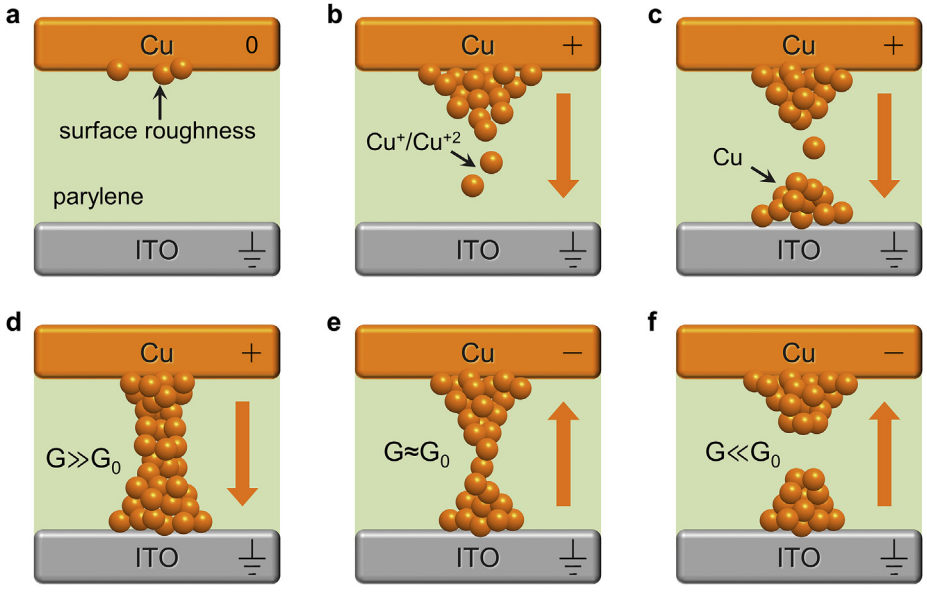

Fig. 4. Schematic evolution of metal bridges (con- ducting filaments) in Cu/PPX/ITO memristors and the consequent quantum conductance effect. (a) Fragment of pristine sandwich structure, having some surface irregularities on the top electrode. The orange pellets represent Cu atoms. (b) A positive voltage is applied to the top electrode of the struc- ture; copper ions begin to move to the cathode (ITO) under the action of an electric field. (c) Copper ions reach the bottom electrode and reduce, so a con- ductive filament begins to grow. (d) The conductive filament has fully formed, quantized conductance is not observed. (e) A negative voltage is applied to the top electrode; copper ions begin to move back- ward to it. A quasi-point contact is

formed, so the conductance is quantized, becoming approximately equal to G_0. (f) The conductive filament has rup- tured; conductance is much less than G_0. (For in- terpretation of the references to colour in this figure legend, the reader is referred to the Web version of this article.)

4. Discussion

According to the results presented above, the RS process in the M/ PPX/ITO structures could be explained by the ECM mechanism: the metal ions of the TE move into the polymer layer under the action of positive voltage, then migrate to the bottom electrode, reducing on it, and form a conducting filament, connecting the upper and lower elec- trodes (see Fig. 4(a–d)). When a negative voltage is applied (Fig. 4(e–f)), the thinnest part of the filament ruptures due to the Joule heating, some of the metal ions return to the TE, and the structure switches to the HRS.

It should also be noted that the I–V curves for the Ag and Cu samples show gradual reset switching, while the Al ones switch more abruptly (see Fig. 1 and S1). This could be explained by taking into account the higher surface activation energy of Cu and Ag compared to Al, which leads to a higher diffusion rate of the latter [31]. This is also the reason why the lifetime of Cu bridges is longer and, hence, the plasticity of Cu samples is better [43]. This assumption is also in accordance with a recent study by Lübben et al. [49], where the filament stability and retention properties of ECM devices were found to be determined by the Gibbs free energy of formation of cations. In particular, this work states that the elements of redox pairs with positive Gibbs free energy (such as Cu and Ag) tend to stay reduced, while the metals of pairs with negative energy (such as Al) tend to oxidize but are difficult to be reduced again. Thus, the best electrode materials identified for ECM switching have free energy slightly above 0 and therefore the redox reactions are easily reversible.

The conductive bridge character of RS is also confirmed by the temperature measurements, from which we see the clear metallic be- havior of R(T) dependence in the LRS. The obtained TCR coefficient $\alpha = (0.62 \pm 0.04) \times 10^{-3}\ K^{-1}$ for the Cu/PPX/ITO devices at 300 K is significantly lower than in the case of the bulk copper, having the TCR of $\alpha \approx 4 \times 10^{-3}\ K^{-1}$, but many studies have shown that the TCR de- creases with the size of metal nanowires [45–47]. Our value of the TCR is also very close to that reported for Cu nanowires with a small dia- meter of ~10 nm ($\alpha \approx 1 \times 10^{-3}\ K^{-1}$) [50]. Thus we may conclude that the metallic behavior of the LRS of Cu/PPX/ITO memristors originates from the conducting Cu filament with the diameter less than 10 nm at its narrowest region. The cross-sectional TEM of the samples also shows a possibility for the metal bridge formation since the Cu/PPX interface is not smooth. The impedance spectroscopy investigations showed that the capacitance of the structures does not change after switching them from HRS to LRS and back, which also supports the ECM nature of RS.

The conductance quantization, observed in the samples using low- speed I–V measurements (0.1 V/s), also supports the filamentary nature of the switching. Moreover, during the measurements we have found a specific quantization effect, namely, that the conductance takes not only integer multiples of the conductance quantum G_0, but also half- integer ones. This result is somewhat unexpected, since only integer conductance quanta are usually observed in ECM memristors [37,38]. But, as already mentioned, in the case of using an organic dielectric in a memristor, half-integer G_0 values can also be observed even in a metal- bridge devices [48,50]. It is also worth mentioning that the con- ductance quantization effect in parylene-based memristors has not been previously reported. Meanwhile, this phenomenon may be useful for the development of innovative computing devices, for example, ultra- high density memory cells [24].

As for the nature of the observed half-integer quantized states of conductance, today it is impossible to give a complete answer to this question. Some works claim, for instance, that they may derive from the adsorbed impurities in the metal bridges, which transforms the con- striction configuration and influences the energy band structure [51]. The possible explanation is the strong interaction between the bridges and the hydrogen component from organic storage media [38]. If we consider the nature of this effect more deeply, we can assume that it may occur because of the spontaneous splitting of the transport elec- trons spin bands due to the Rashba effect [52,53]. In general, analysis of related literature reveals that the question about the nature of half-in- teger conductance states in such systems is a bit speculative and the underlying physical mechanism remains unclear. And although this question is extremely interesting, its detailed analysis lies obviously beyond the scope of this study.

5. Conclusions

In conclusion, we attribute the bipolar resistive switching phe- nomenon in the M/PPX/ITO structures to the formation and rupture of metal (Cu, Ag and Al) filaments when a positive and negative voltage is applied to the top electrode, respectively (the so-called electrochemical metallization mechanism). This is confirmed by the temperature de- pendence of the resistance as well as by impedance spectroscopy ex- periments. By slowing down the voltage sweep speed in the I–V mea- surements, conductance quantization with both integer and half-integer multiples of G_0 is observed. Considering the fact that the samples have an organic dielectric layer, and the recent literature data, this result also confirms the metallic filament hypothesis. The results obtained, along with those we obtained earlier [43], give every reason to consider the parylene-based memristors as promising building blocks of in- novative computing systems such as hardware neural networks or multi-level data storage devices.

References

[1] D. Ielmini, Resistive switching memories based on metal oxides: mechanisms, re- liability and scaling, Semicond. Sci. Technol. 31 (2016) 063002https://doi.org/10. 1088/0268-1242/31/6/063002.

[2] D. Ielmini, H.-S.P. Wong, In-memory computing with resistive switching devices, Nat. Electron. 1 (2018) 333–343 https://doi.org/10.1038/s41928-018-0092-2.

[3] J. Del Valle, J.G. Ramírez, M.J. Rozenberg, I.K. Schuller, Challenges in materials and devices for resistive-switching-based neuromorphic computing, J. Appl. Phys. 124 (2018) 211101 https://doi.org/10.1063/1.5047800.

[4] Y. Li, Z. Wang, R. Midya, Q. Xia, J.J. Yang, Review of memristor devices in neu- romorphic computing: materials sciences and device challenges, J. Phys. D Appl. Phys. 51 (2018) 503002 https://doi.org/10.1088/1361-6463/aade3f.

[5] F. Merrikh Bayat, M. Prezioso, B. Chakrabarti, H. Nili, I. Kataeva, D. Strukov, Implementation of multilayer perceptron network with highly uniform passive memristive crossbar circuits, Nat. Commun. 9 (2018) 2331 https://doi.org/10. 1038/s41467-018-04482-4.

[6] A.N. Mikhaylov, O.A. Morozov, P.E. Ovchinnikov, I.N. Antonov, A.I. Belov,
D.S. Korolev, A.N. Sharapov, E.G. Gryaznov, O.N. Gorshkov, Y.I. Pigareva,
A.S. Pimashkin, S.A. Lobov, V.B. Kazantsev, One-board design and simulation of double-layer perceptron based on metal-oxide memristive nanostructures, IEEE Trans. Emerg. Topics Comput. Intell. 2 (2018) 371–379 https://doi.org/10.1109/ TETCI.2018.2829922.

[7] Y.VandeBurgt,A.Melianas,S.T.Keene,G.Malliaras,A.Salleo,Organicelectronics for neuromorphic computing, Nat. Electron. 394 (2018) 386–397 https://doi.org/10.1038/s41928-018-0103-3.

[8] N.R. Hosseini, J.-S. Lee, Biocompatible and flexible chitosan-based resistive switching memory with magnesium electrodes, Adv. Funct. Mater. 25 (2015) 5586–5592 https://doi.org/10.1002/adfm.201502592.

[9] G.U. Siddiqui, M.M. Rehman, Y.J. Yang, K.H. Choi, A two-dimensional hexagonal boron nitride/polymer nanocomposite for flexible resistive switching devices, J. Mater. Chem. C 5 (2017) 862–871 https://doi.org/10.1039/C6TC04345C.

[10] Q. Xia, J.J. Yang, Memristive crossbar arrays for brain-inspired computing, Nat. Mater. 18 (2019) 309–323 https://doi.org/10.1038/s41563-019-0291-x.

[11] M. Hamaguchi, K. Aoyama, S. Asanuma, Y. Uesu, T. Katsufuji, Electric-field induced resistance switching universally observed in transition-metal-oxide thin films, Appl. Phys. Lett. 88 (2006) 142508 https://doi.org/10.1063/1.2193328.

[12] S.U. Sharath, J. Kurian, P. Komissinskiy, E. Hildebrandt, T. Bertaud, C. Walczyk, P. Calka, T. Schroeder, L. Alff, Thickness independent reduced forming voltage in oxygen engineered HfO_2 based resistive switching memories, Appl. Phys. Lett. 105 (2014) 073505https://doi.org/10.1063/1.4893605.

[13] Y. Wang, K. Chen, X. Qian, Z. Fang, W. Li, J. Xu, The x dependent two kinds of resistive switching behaviors in SiO_x films with different x component, Appl. Phys. Lett. 104 (2014) 012112https://doi.org/10.1063/1.4861592.

[14] Y.H. Wang, K.H. Zhao, X.L. Shi, G.L. Xie, S.Y. Huang, L.W. Zhang, Investigation of the resistance switching in Au/$SrTiO_3$:Nb heterojunctions, Appl. Phys. Lett. 103 (2013) 031601https://doi.org/10.1063/1.4813622.

[15] J.J. Yang, M.-X. Zhang, J.P. Strachan, F. Miao, M.D. Pickett, R.D. Kelley,
G. Medeiros-Ribeiro, R.S. Williams, High switching endurance in TaOx memristive devices, Appl. Phys. Lett. 97 (2010) 232102 https://doi.org/10.1063/1.3524521.

[16] A. Mehonic, A.L. Shluger, D. Gao, I. Valov, E. Miranda, D. Ielmini, A. Bricalli,
E. Ambrosi, C. Li, J.J. Yang, Q. Xia, A.J. Kenyon, Silicon oxide (SiOx): a promising material for resistance switching? Adv. Mater. 30 (2018) 1801187 https://doi.org/10.1002/adma.201801187.

[17] A.N. Mikhaylov, A.I. Belov, D.V. Guseinov, D.S. Korolev, I.N. Antonov,
D.V. Efimovykh, S.V. Tikhov, A.P. Kasatkin, O.N. Gorshkov, D.I. Tetelbaum,
A.I. Bobrov, N.V. Malekhonova, D.A. Pavlov, E.G. Gryaznov, A.P. Yatmanov, Bipolar resistive switching and charge transport in silicon oxide memristor, Mater. Sci. Eng., B 194 (2015) 48–54 https://doi.org/10.1016/j.mseb.2014.12.029.

[18] S. Kim, B.-G. Park, Nonlinear and multilevel resistive switching memory in Ni/ Si3N4/Al2O3/TiN structures, Appl. Phys. Lett. 108 (2016) 212103 https://doi.org/ 10.1063/1.4952719.

[19] V.A. Demin, V.V. Erokhin, A.V. Emelyanov, S. Battistoni, G. Baldi, S. Iannotta, P.K. Kashkarov, M.V. Kovalchuk, Hardware elementary perceptron based on poly-aniline memristive devices, Org. Electron. 25 (2018) 16–20 https://doi.org/10. 1016/j.orgel.2015.06.015.

[20] D.A. Lapkin, A.V. Emelyanov, V.A. Demin, V.V. Erokhin, L.A. Feigin,
P.K. Kashkarov, M.V. Kovalchuk, Polyaniline-based memristive microdevice with high switching rate and endurance, Appl. Phys. Lett. 112 (2018) 043302https://doi. org/10.1063/1.5013929.

[21] B.C. Das, R.G. Pillai, Y. Wu, R.L. McCreery, Redox-gated three-terminal organic memory devices: effect of composition and environment on performance, ACS Appl. Mater. Interfaces 5 (2013) 11052–11058 https://doi.org/10.1021/am4032828.

[22] T.-Y. Wang, Z.-Y. He, H. Liu, L. Chen, H. Zhu, Q.-Q. Sun, S.-J. Ding, P. Zhou, D.W. Zhang, Flexible electronic synapses for face recognition application with multimodulated conductance states, ACS Appl. Mater. Interfaces 10 (2018) 37345–37352 https://doi.org/10.1021/acsami.8b16841.

[23] V.V. Rylkov, S.N. Nikolaev, V.A. Demin, A.V. Emelyanov, A.V. Sitnikov,
K.E. Nikiruy, V.A. Levanov, M.Yu Presnyakov, A.N. Taldenkov, A.L. Vasiliev, K.Yu Chernoglazov, A.S. Vedeneev, YuE. Kalinin, A.B. Granovsky, V.V. Tugushev, A.S. Bugaev, Transport, magnetic, and memristive properties of a nanogranular $(CoFeB)_x(LiNbO_y)_{100-x}$ composite material, J. Exp. Theor. Phys. 126 (2018) 353–367 https://doi.org/10.1134/S1063776118020152.

[24] S. Gao, F. Zeng, C. Chen, G. Tang, Y. Lin, Z. Zheng, C. Song, F. Pan, Conductance quantization in a Ag filament-based polymer resistive memory, Nanotechnology 24 (2013) 335201 https://doi.org/10.1088/0957-4484/24/33/335201.

[25] M.N. Awais, K.H. Choi, Memristive behavior in electrohydrodynamic atomized layers of poly[2-methoxy-5-(2′-ethylhexyloxy)–(p -phenylenevinylene)] for next generation printed electronics, Jpn. J. Appl. Phys. 52 (2013) 05DA05https://doi. org/10.7567/JJAP.52.05DA05.

[26] M.N. Awais, K.H. Choi, Resistive switching in a printed nanolayer of poly(4-vi- nylphenol), J. Electron. Mater. 42 (2013) 1202–1208 https://doi.org/10.1007/s11664-013-2560-9.

[27] Y. Busby, S. Nau, S. Sax, E.J.W. List-Kratochvil, J. Novak, R. Banerjee, F. Schreiber, J.-J. Pireaux, Direct observation of conductive filament formation in Alq_3 based organic resistive memories, J. Appl. Phys. 118 (2015) 075501https://doi.org/10. 1063/1.4928622.

[28] N. Raeis Hosseini, J.-S. Lee, Resistive switching memory based on bioinspired natural solid polymer electrolytes, ACS Nano 9 (2015) 419–426 https://doi.org/10. 1021/nn5055909.

[29] K. Krishnan, T. Tsuruoka, C. Mannequin, M. Aono, Mechanism for conducting fi- lament growth in self-assembled polymer thin films for redox-based atomic switches, Adv. Mater. 28 (2016) 640–648 https://doi.org/10.1002/adma. 201504202.

[30] B. Sun, X. Zhang, G. Zhou, P. Li, Y. Zhang, H. Wang, Y. Xia, Y. Zhao, An organic nonvolatile resistive switching memory device fabricated with natural pectin from fruit peel, Org. Electron. 42 (2017) 181–186 https://doi.org/10.1016/j.orgel.2016. 12.037.

[31] W. Wang, M. Wang, E. Ambrosi, A. Bricalli, M. Laudato, Z. Sun, X. Chen, D. Ielmini, Surface diffusion-limited lifetime of silver and copper nanofilaments in resistive switching devices, Nat. Commun. 10 (2019) 81 https://doi.org/10.1038/s41467- 018-07979-0.

[32] W.-J. Joo, T.L. Choi, K.H. Lee, Y. Chung, Study on threshold behavior of operation voltage in metal filament-based polymer memory, J. Phys. Chem. B 111 (2007) 7756–7760 https://doi.org/10.1021/jp0684933.

[33] Y.-C. Chang, Y.-H. Wang, Resistive switching behavior in gelatin thin films for nonvolatile memory application, ACS Appl. Mater. Interfaces 6 (2014) 5413–5421 https://doi.org/10.1021/am500815n.

[34] M.S. Kotova, K.A. Drozdov, T.V. Dubinina, E.A. Kuzmina, L.G. Tomilova,
R.B. Vasiliev, A.O. Dudnik, L.I. Ryabova, D.R. Khokhlov, In situ impedance spec- troscopy of filament formation by resistive switches in polymer based structures, Sci. Rep. 8 (2018) 9080 https://doi.org/10.1038/s41598-018-27332-1.

[35] Y. Luo, D. Zhao, Y. Zhao, F. Chiang, P. Chen, M. Guo, N. Luo, X. Jiang, P. Miao, Y. Sun, A. Chen, Z. Lin, J. Li, W. Duan, J. Caib, Y. Wang, Evolution of Ni nanofi- laments and electromagnetic coupling in the resistive switching of NiO, Nanoscale 7 (2015) 642–649 https://doi.org/10.1039/c4nr04394d.

[36] H. Ohnishi, Y. Kondo, K. Takayanagi, Quantized conductance through individual rows of suspended gold atoms, Nature 395 (1998) 780–783 https://doi.org/10.

1038/27399.

[37] A. Mehonic, A. Vrajitoarea, S. Cueff, S. Hudziak, H. Howe, C. Labbe, R. Rizk, M. Pepper, A.J. Kenyon, Quantum conductance in silicon oxide resistive memory devices, Sci. Rep. 3 (2013) 2708 https://doi.org/10.1038/srep02708.

[38] W. Xue, S. Gao, J. Shang, X. Yi, G. Liu, R.-W. Li, Recent advances of quantum conductance in memristors, Adv. Electron. Mater (2019) 1800854 https://doi.org/10.1002/aelm.201800854.

[39] Y. Cai, J. Tan, L. Ye Fan, M. Lin, R. Huang, A flexible organic resistance memory device for wearable biomedical applications, Nanotechnology 27 (2016) 275206 https://doi.org/10.1088/0957-4484/27/27/275206.

[40] Q. Chen, M. Lin, Z. Wang, X. Zhao, Y. Cai, Q. Liu, Y. Fang, Y. Yang, M. He, R. Huang, Low power parylene-based memristors with a graphene barrier layer for flexible electronics applications, Adv. Electron. Mater (2019) 1800852 https://doi.org/10. 1002/aelm.201800852.

[41] S. Song, J. Jang, Y. Ji, Twistable nonvolatile organic resistive memory devices, Org. Electron. 14 (2013) 2087–2092 https://doi.org/10.1016/j.orgel.2013.05.003.

[42] D. Son, S. Qiao, R. Ghaffari, Multifunctional wearable devices for diagnosis and therapy of movement disorders, Nat. Nanotechnol. 9 (2014) 397–404 https://doi. org/10.1038/nnano.2014.38.

[43] A.A. Minnekhanov, A.V. Emelyanov, D.A. Lapkin, K.E. Nikiruy, B.S. Shvetsov, A.A. Nesmelov, V.V. Rylkov, V.A. Demin, V.V. Erokhin, Parylene Based Memristive Devices with Multilevel Resistive Switching for Neuromorphic Applications, (2019) arXiv:1901.08667 [physics.app-ph] (preprint) https://arxiv.org/abs/1901.08667.

[44] G.C. Adam, A. Khiat, T. Prodromakis, Challenges hindering memristive neuro- morphic hardware from going mainstream, Nat. Commun. 9 (2018) 5267 https:// doi.org/10.1038/s41467-018-07565-4.

[45] W. Guan, M. Liu, S. Long, Q. Liu, W. Wang, On the resistive switching mechanisms of Cu/ZrO2:Cu/Pt, Appl. Phys. Lett. 93 (2008) 22 https://doi.org/10.1063/1.

3039079.

[46] A. Bid, A. Bora, A.K. Raychaudhuri, Temperature dependence of the resistance of metallic nanowires of diameter 15 nm: applicability of Bloch-Grüneisen theorem, Phys. Rev. B 74 (2006) 035426https://doi.org/10.1103/PhysRevB.74.035426.

[47] Y. Zhao, Z. Zhang, Y. Zhang, Y. Li, Z. He, Z. Yan, Large-scale synthesis of Cu na-nowires with gradient scales by using “hard” strategies and size effects on electrical properties, CrystEngComm 15 (2013) 332–342 https://doi.org/10.1039/ C2CE26508G.

[48] K. Krishnan, M. Muruganathan, T. Tsuruoka, H. Mizuta, M. Aono, Highly re- producible and regulated conductance quantization in a polymer-based atomic switch, Adv. Funct. Mater. 27 (2017) 1605104 https://doi.org/10.1002/adfm. 201605104.

[49] M. Lübben, I. Valov, Active electrode redox reactions and device behavior in ECM type resistive switching memories, Adv. Electron. Mater (2019) 1800933 https:// doi.org/10.1002/aelm.201800933.

[50] S. Gao, C. Song, C. Chen, F. Zeng, F. Pan, Dynamic processes of resistive switching in metallic filament-based organic memory devices, J. Phys. Chem. C 116 (2012) 17955–17959 https://doi.org/10.1021/jp305482c.

[51] Y. Sun, D. Wen, Conductance quantization in nonvolatile resistive switching memory based on the polymer composite of zinc oxide nanoparticles, J. Phys. Chem. C 122 (2018) 10582–10591 https://doi.org/10.1021/acs.jpcc.8b01120.

[52] O. Goulko, F. Bauer, J. Heyder, J. von Delft, Effect of spin-orbit interactions on the 0.7 anomaly in quantum point contacts, Phys. Rev. Lett. 113 (2014) 266402 https://doi.org/10.1103/PhysRevLett.113.266402.

[53] R. Cuan, L. Diago-Cisneros, Hole spectra and conductance for quantum wire systems under Rashba spin-orbit interaction, J. Appl. Phys. 110 (2011) 113705 https://doi. org/10.1063/1.3660213.